

Electronic Supplementary Information

An Mo-salicylaldehyde-linker (Mo-Tp) based 2D MOF as a single-atom catalyst for the nitrogen reduction reaction.

Hassan A. Alhadidi Almheiri,^{ad} Nirpendra Singh^{bd}, Dinesh Shetty^{*cd} Kyriaki Polychronopoulou^{de},
and Ali A. Alhammad^{i* ad}

^a Department of Chemical Engineering, Khalifa University of Science and Technology, P.O Box 127788 Abu Dhabi, United Arab Emirates

^b Department of Physics, Khalifa University of Science and Technology, P.O Box 127788 Abu Dhabi, United Arab Emirates

^c Department of Chemistry, Khalifa University of Science and Technology, P.O Box 127788 Abu Dhabi, United Arab Emirates

^d Center of Catalysis and Separation, Khalifa University of Science and Technology, Main Campus, Abu Dhabi, United Arab Emirates.

^e Mechanical Engineering Department, Khalifa University of Science and Technology, Main Campus, Abu Dhabi, P.O. Box 127788, United Arab Emirates.

Note S1: Electrochemical reaction calculations.

The free energies were calculated using the computational hydrogen electrode (CHE) model [S1] as:

$$\Delta G = \Delta E + \Delta E_{ZPE} - T\Delta S + \Delta G_U + \Delta G_{pH}$$

Where ΔE is the energy difference, ΔE_{ZPE} is the zero-point energy (ZPE), T is the temperature, ΔS is the entropy difference ($S=S_{vib}$), $\Delta G_U = eU$ (e is the electrode transfer and U is the electrode potential), and $\Delta G_{pH} = k_B T \times \ln 10 \times pH$ (k_B is the Boltzmann constant).

Phonon calculations were carried out using the finite difference method to obtain the values of vibrational frequencies. The zero-point energy (ZPE) and the vibrational entropy (S_{vib}) are computed through equations 1 and 2 for each of the reaction intermediates [S2]. In equations 1 and 2, θ_{vi} is known as the characteristic vibrational temperature equal to $h\nu_i/k_B$, T is the absolute temperature (300 K), h is Plank's constant, k_B is Boltzmann's constant, R is the molar gas constant, and ν_i is the vibrational frequency. The fluctuations caused by interchanging the metal atoms are neglected, because only the surface intermediate species are allowed to vibrate while the surface atoms are kept fixed. The estimated values of the zero-point energy (E_{ZPE}) and entropic contributions (TS_{vib}) for all the adsorption species are summarized in table ES5. The NIST database [S3] is used to retrieve vibrational frequencies of the gaseous species.

$$E_{ZPE} = \sum_i \frac{1}{2} h\nu_i$$

Equation 1

$$S_{vib} = R \sum_i \left(\frac{\frac{\theta_{vi}}{T}}{\exp\left(\frac{\theta_{vi}}{T}\right) - 1} - \ln \left[1 - \exp\left(\frac{-\theta_{vi}}{T}\right) \right] \right)$$

Equation 2

Supplementary Figures

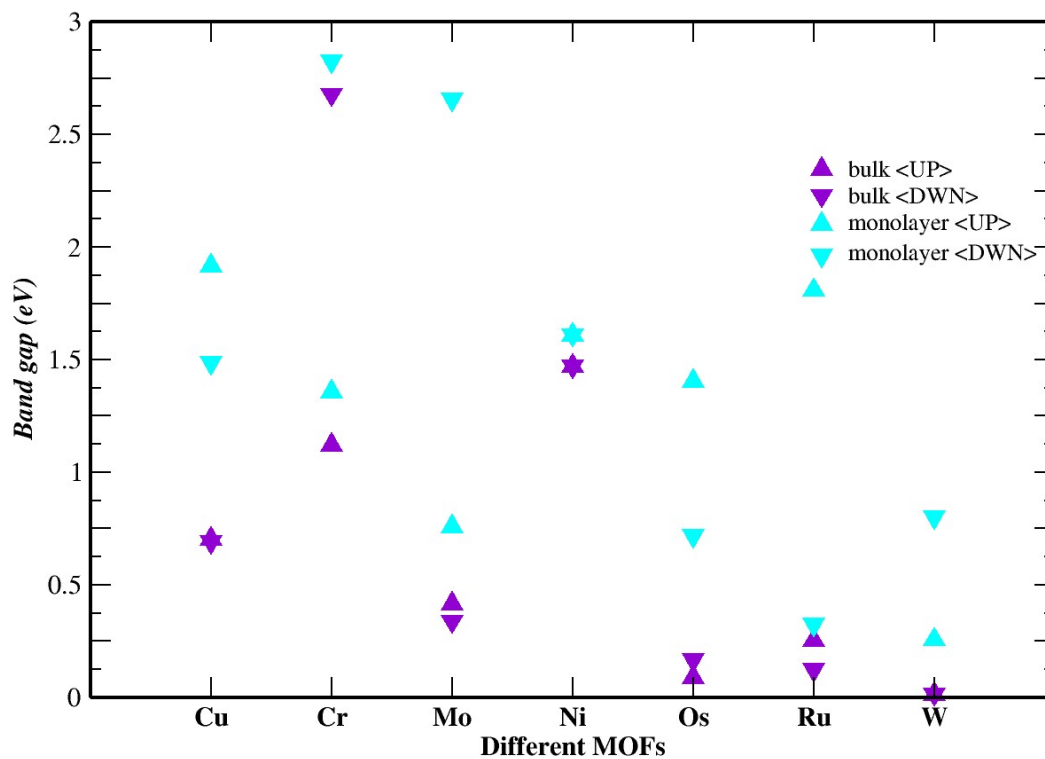


Figure S1: The values of the band gap in different TM-Tp MOFs [TM = Cu, Ni, Cr, Mo, Os, Ru, and W] in both bulk and monolayer structures. The bandgaps are decomposed into spin-up <UP> and spin-down <DOWN> states due to using spin-polarized calculations and DFT+U.

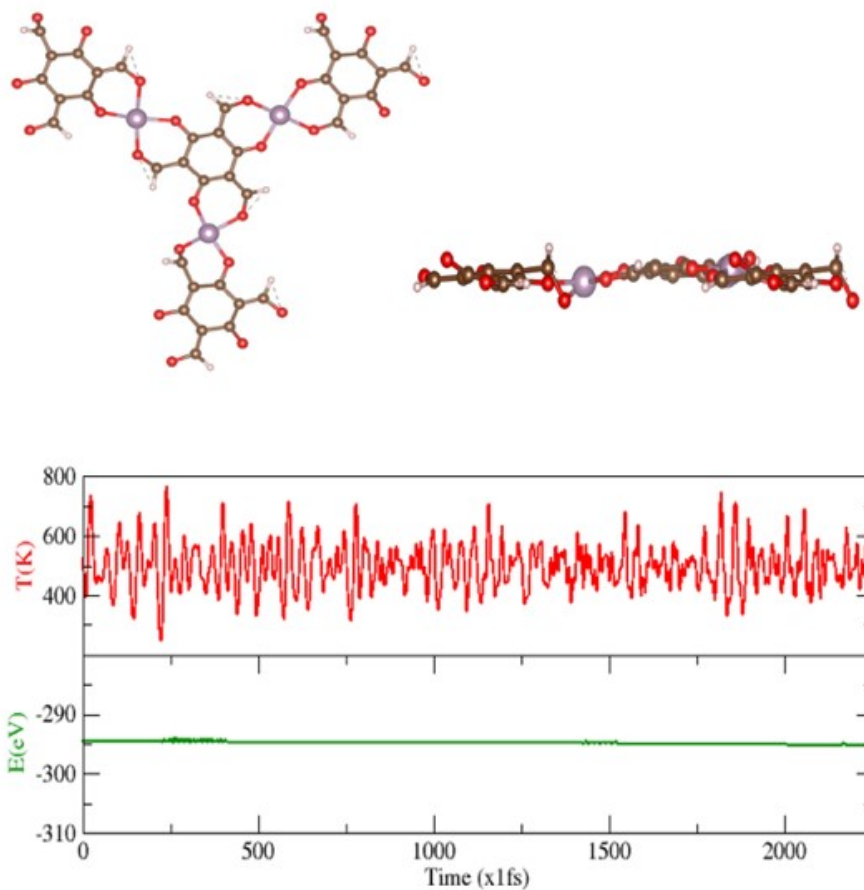


Figure S2: Results of the ab initio molecular dynamics (AIMD) simulation at 500K showing the variation of the energy and temperature. Additionally, shown is also the top and side view of the final structure after the AIMD run.

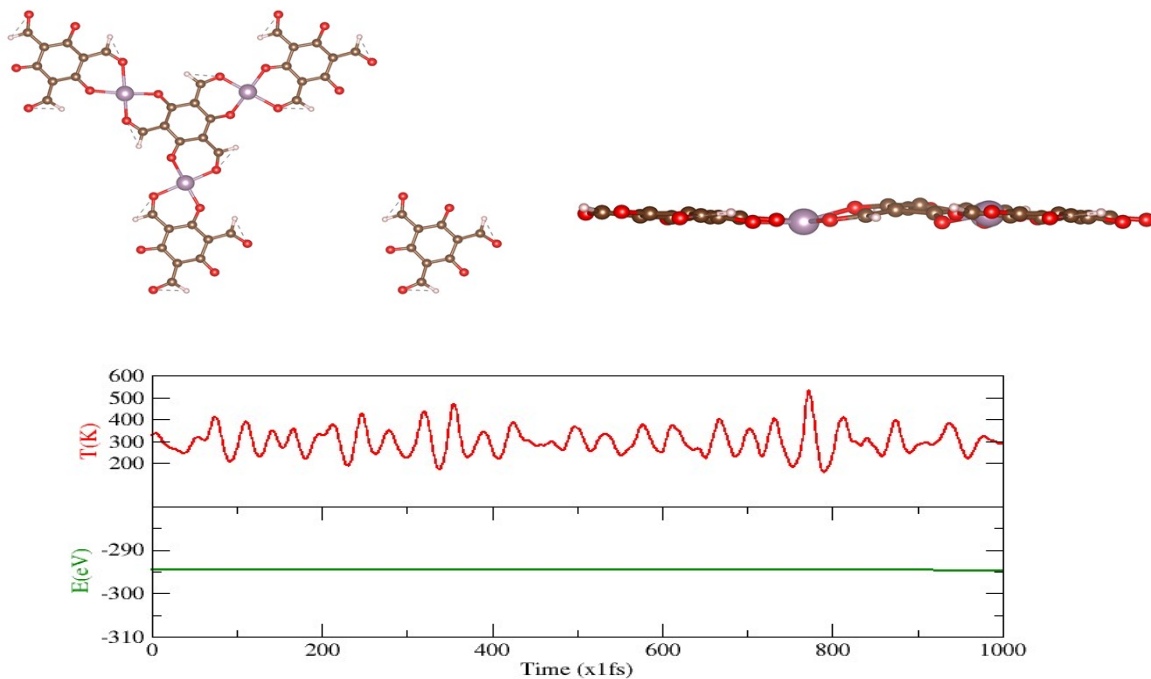


Figure S3: Results of the ab initio molecular dynamics (AIMD) simulation at 300K showing the variation of the energy and temperature. Additionally, shown is also the top and side view of the final structure after the AIMD run.

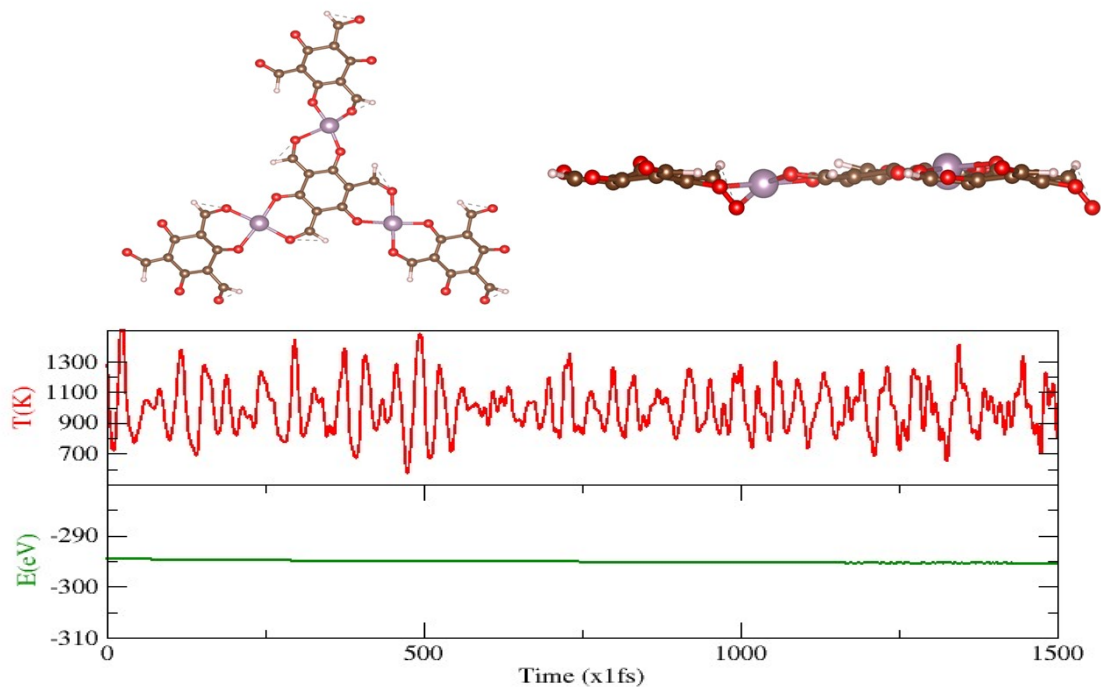


Figure S4: Results of the ab initio molecular dynamics (AIMD) simulation at 1000K showing the variation of the energy and temperature. Additionally, shown is also the top and side view of the final structure after the AIMD run.

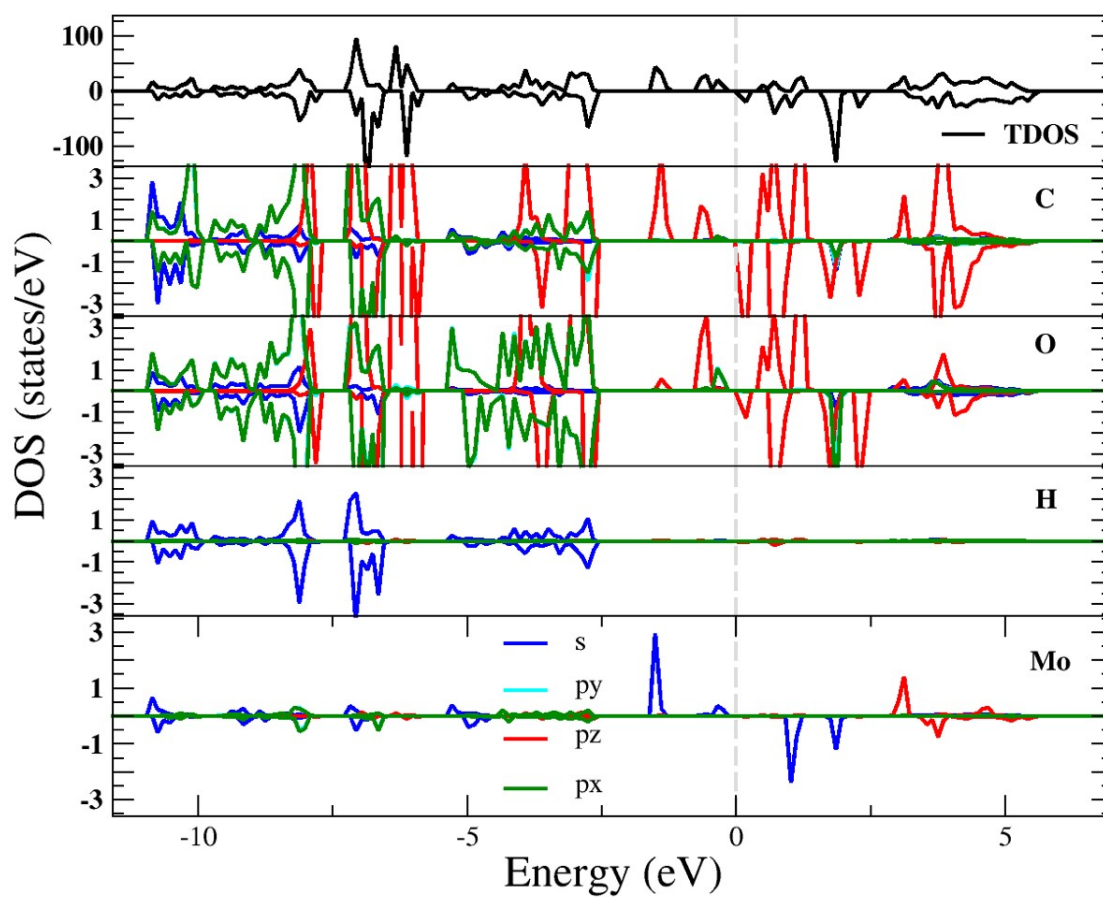
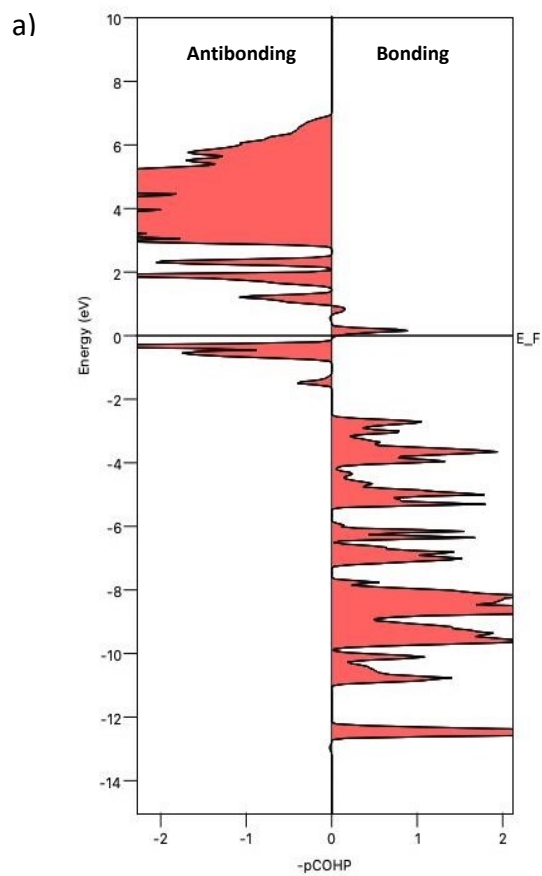


Figure S5: Density of states plot showing the total density of states (TDOS) and projected Density of states (pDOS) of Mo, C, O, and H in our Mo-Tp MOF monolayer.

Mo-O (O-C-H)



Mo-N (*NNH)

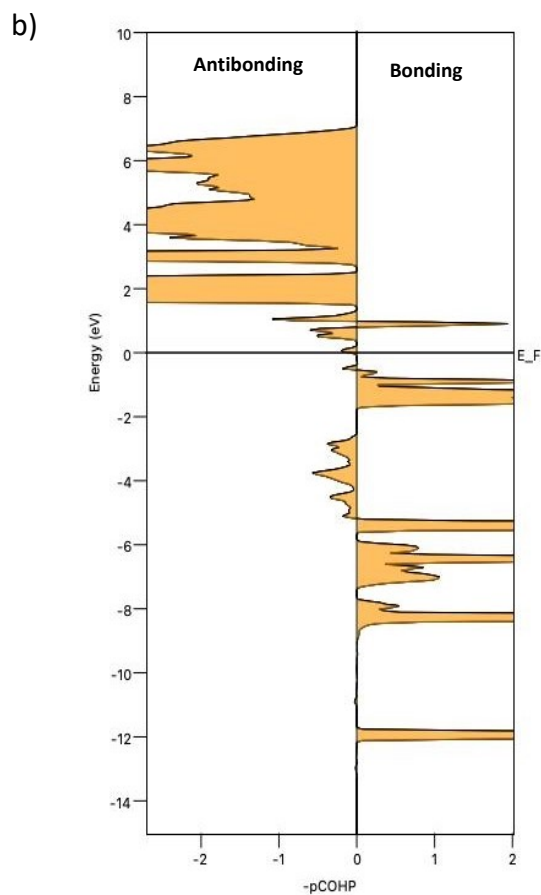


Figure S6: Projected crystal orbital Hamiltonian populations (pCOHP) analysis between a) Mo and the O atom connected to the methoxy group (O-C-H) b) between Mo and the nearest N atom in the NNH intermediate. -ICOHP and charge spilling values are summarized in table S7.

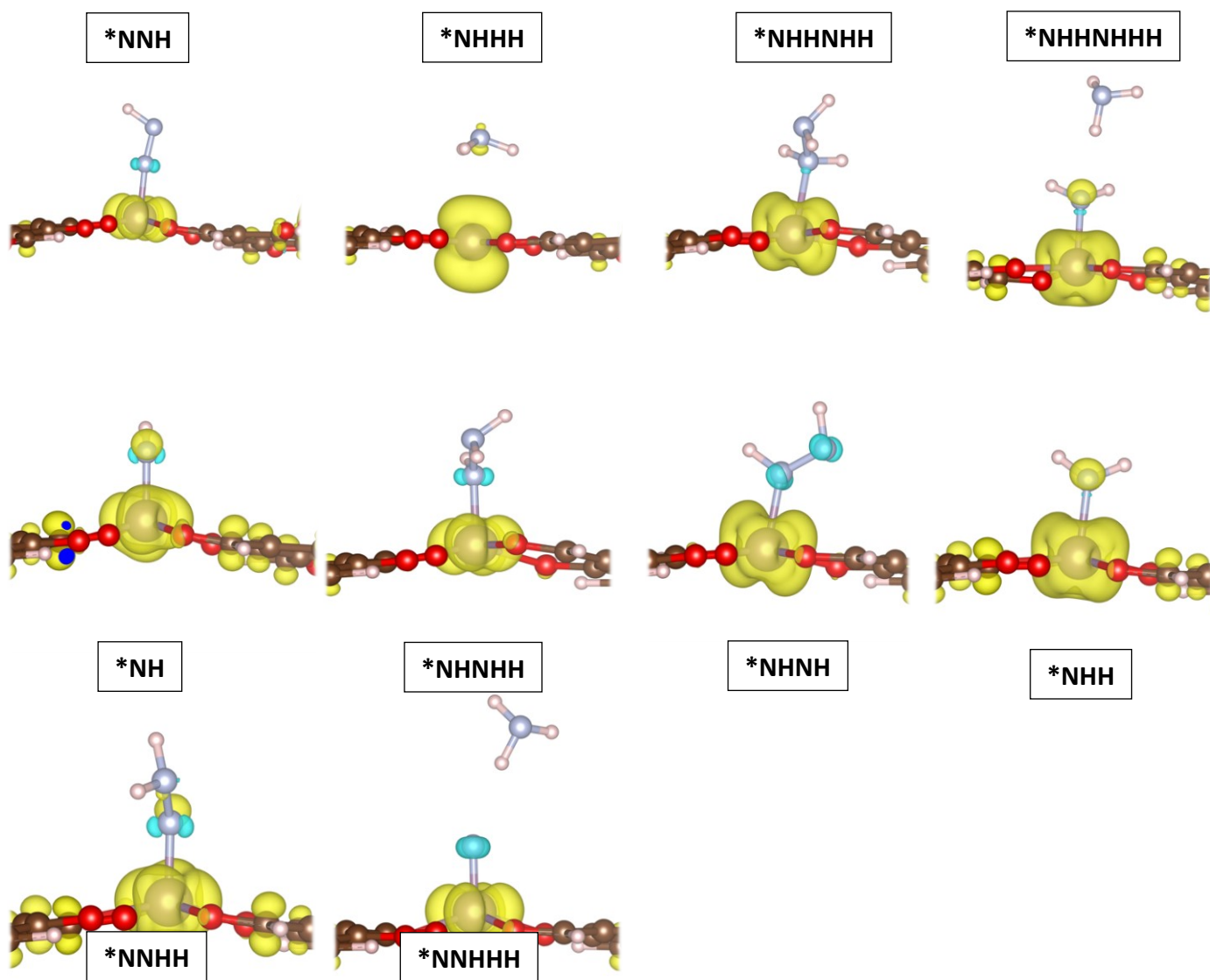


Figure S7: Spin density of NRR intermediates. Spin-up density is shown in yellow while spin-down density is shown in blue.

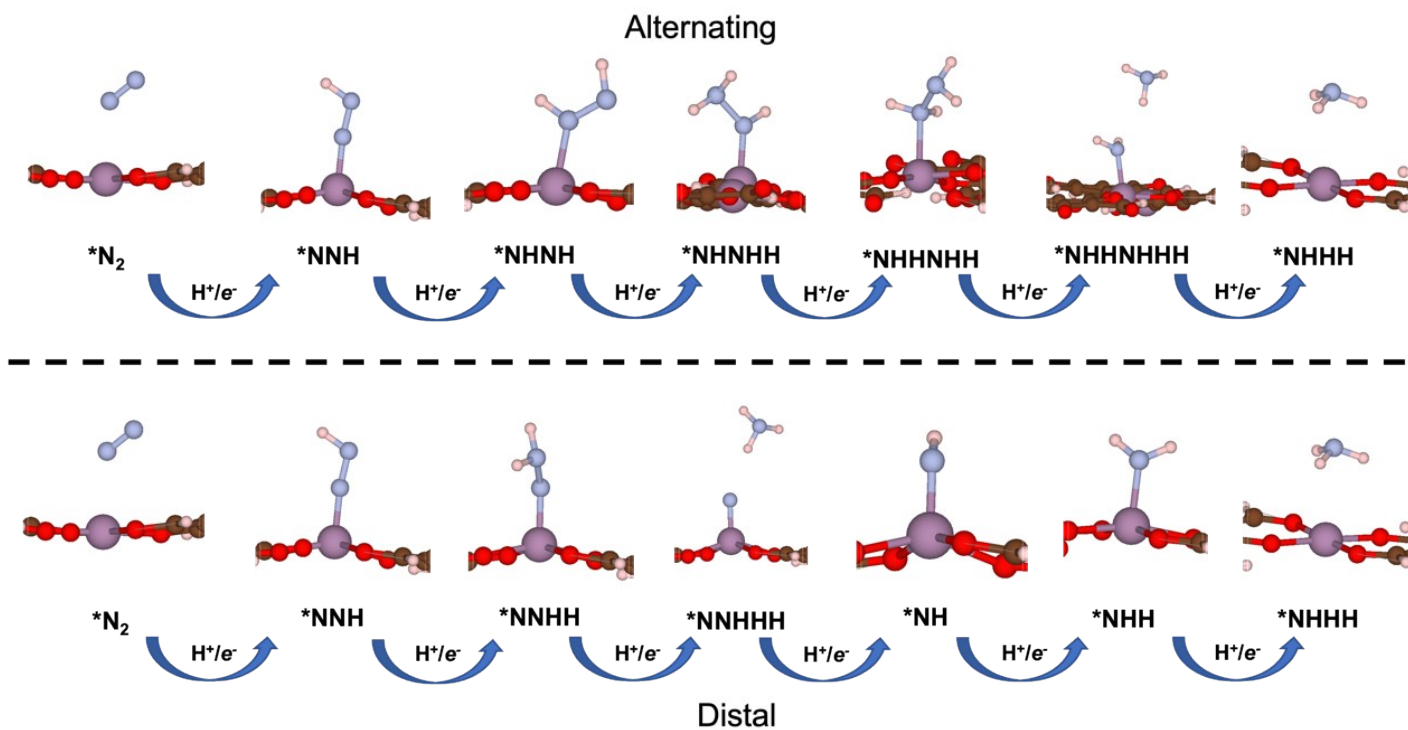


Figure S8: Schematic of the possible NRR reaction pathways with their corresponding NRR intermediates on the Mo-Tp MOF monolayer.

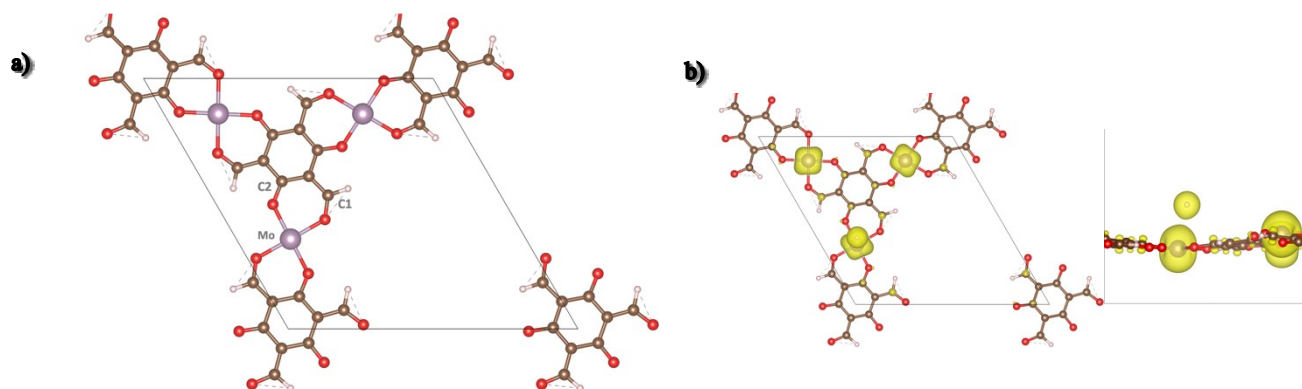


Figure S9: a) A schematic of the selected adsorption sites Mo, C1, and C2 for the selectivity analysis. b) Top and side view of the spin density of $*\text{H}/\text{Mo-Tp}$ MOF monolayer system. Spin-up density is shown in yellow while spin-down density is in blue. Isosurfaces are set to 0.10 a.u

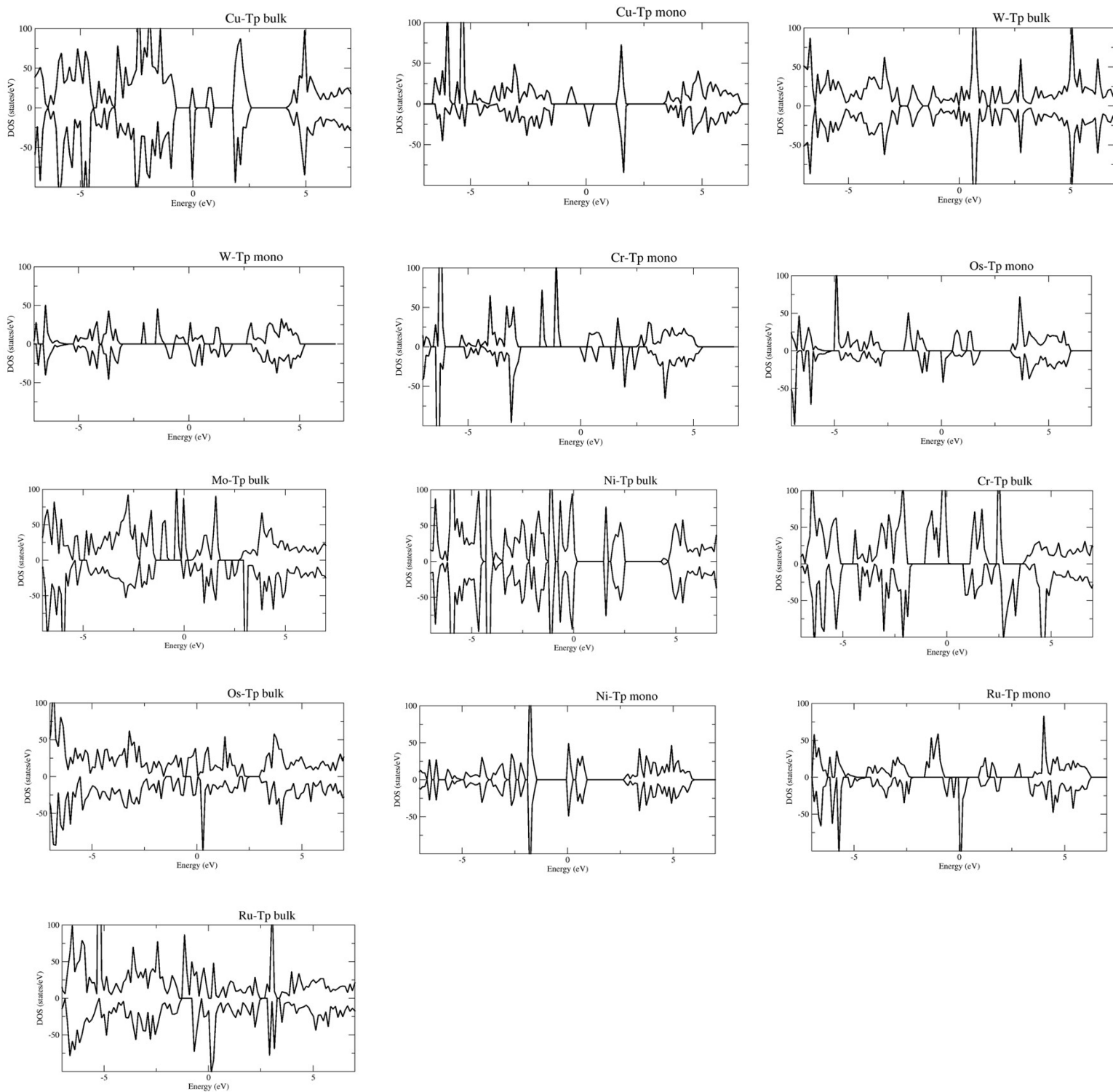


Figure S10: Density of states (DOS) plots of all TM-Tp bulk and monolayer systems studied in this work.

Supplementary Tables

Table S1: Bulk optimized lattice parameters

Lattice parameters (Å)						
Metal	a	b	c	n	D _{pore}	(TM-O) avg
Cu	14.67286	14.67286	9.70718	3.67	13.22677	1.9288225
Ni	14.43425	14.43425	9.94704	3.78	12.97455	1.8461275
Cr	14.8669	14.8669	9.71977	3.70	13.47732	1.9529
Mo	15.12631	15.12631	10.03189	3.33	13.73955	2.059555
Os	14.86969	14.86969	9.68544	3.14	13.4583	1.9485
Ru	14.83384	14.83384	9.76112	3.19	13.34515	1.946305
W	15.05927	15.05927	9.16618	3.04	14	1.9519175

Table S2: Magnetic moment and d-band center energy levels in different TM-Tp monolayer systems. D-band centers are composed into spin-up (ϵ_{\uparrow}) and spin-down (ϵ_{\downarrow}) d-band centers. E_{exf} denotes exfoliation energies required to isolate a single layer from the bulk.

TM-Tp MOF monolayer system	E_{exf} (meV/Å ²)	Magnetic moment (μ_{B})	ϵ_{\uparrow} (eV)	ϵ_{\downarrow} (eV)
Cu -Tp	13.3	3	-3.301	-2.506
Ni-Tp	12.7	0	-2.417	-2.416
Cr-Tp	13.9	12	-1.809	1.227
Mo-Tp	44.0	12	-1.861	0.642
Os-Tp	20.6	6	-2.285	-1.371
Ru-Tp	17.6	6	-1.466	-0.8
W-Tp	27.1	6	-3.51	-1.993

Table S3: End-on and side-on calculated N₂ adsorption energies (ΔE_{N_2}), N₂ adsorption free energy (ΔG_{N_2}), N-N bond length (L_{N-N}), and distance between transition metal and nearest N atom (D_{TM-N}).

TM-Tp MOF system	End -on				Side-on			
	ΔE_{N_2} (eV)	ΔG_{N_2} (eV)	L_{N-N} (Å)	D_{TM-N} (Å)	ΔE_{N_2} (eV)	ΔG_{N_2} (eV)	L_{N-N} (Å)	D_{TM-N} (Å)
Cu -Tp	-0.081	0.224	1.11336	3.17388	-0.01	0.5	1.11353	6.39698
Cr-Tp	-0.052	0.253	1.11339	3.20535	-0.01	0.5	1.11355	6.42966
Mo-Tp	-0.135	0.17	1.12416	2.56761	-0.01	0.5	1.11367	6.68034
Ni-Tp	-0.096	0.209	1.11405	3.26684	-0.01	0.5	1.11362	6.39728
Os-Tp	-0.032	0.273	1.11372	4.4765	-0.012	0.498	1.11361	6.30976
Ru-Tp	0.649	0.954	1.11372	4.39162	0.089	0.599	1.11363	6.23949
W-Tp	-0.066	0.239	1.11373	3.50765	-0.012	0.498	1.11363	6.47219

Table S4: End-on calculated *NNH adsorption energies (ΔE_{*NNH}), NNH adsorption free energy (ΔG_{*NNH}), N-N bond length (L_{N-N}), and distance between transition metal and nearest N atom (D_{TM-N}).

TM-Tp MOF system	End -on			
	ΔE_{*NNH} (eV)	ΔG_{*NNH} (eV)	L_{N-N} (Å)	D_{TM-N} (Å)
Cr-Tp	-1.442	-0.615	3.05969	1.18145
Mo-Tp	-3.511	-2.684	1.78407	1.23897
Ni-Tp	-0.563	0.264	2.099	1.18328

Table S5: Zero-point energy corrections (ΔE_{ZPE}) and entropic contributions ($T\Delta S$; T at 300K) to the free energies of the adsorbate species and gaseous species. Considered on Mo-Tp MOF monolayer (*) and estimated from the vibrational frequencies.

Species	ΔE_{ZPE} (eV)	$T\Delta S$ (eV)
N₂(g)	0.15	0.59
*NN	0.17	0.305
*N*N	0.124	0.0234
*NNH	0.519	0.132
*H₂(g)	0.27	0.41
*NH₃(g)	0.58	0.56
*H	0.031	0.0126
*NHNH	0.831	0.262
*NHNHH	1.15	0.405
*NHHNHH	1.509	0.373
*NHHNHHH	1.6	0.263
*NHHH	0.944	0.261
*NHH	0.651	0.126
*NH	0.324	0.265
*NNHHH	1.06	0.338
*NNHH	0.817	0.126

Table S6: First two columns show the N-N bond length (L_{N-N}) and the distance between transition metal and nearest N atom (D_{TM-N}) of different adsorbate/Mo-Tp monolayer systems. The next four columns show the conducted bader charge analysis on the different moieties that compose the adsorbate/Mo-Tp MOF monolayer (Q_{xx}). Finally, the last column shows the magnetic moment in different adsorbate/Mo-Tp monolayer systems.

Systems	L_{N-N} (Å)	D_{TM-N} (Å)	Q_{Mo} (e)	$Q_{O_4C_2H_2}$ (e)	$Q_{graphene}$ (e)	Q_{ads} (e)	Magnetic moment (μ_B)
Mo-Tp	-	-	-1.405	1.716	-4.230	-	12.001
*NN/Mo-Tp	1.124	2.564	-1.500	2.841	-7.561	0.140	11.994
*NNH/Mo-Tp	1.238	1.784	-1.829	2.753	-8.258	0.535	9
*NHH/Mo-Tp	1.295	1.964	-1.755	2.837	-4.183	0.258	10.002
*NHHH/Mo-Tp	1.416	1.900	-1.808	2.837	-4.055	0.127	9.002
*NHHHH/Mo-Tp	1.455	2.156	-1.689	2.976	-4.037	-0.235	9.997
*NHHHHH/Mo-Tp	3.283	1.992	-1.825	2.841	-4.196	0.366	11.001
*NHHH/Mo-Tp	-	3.075	-1.578	2.898	-4.088	-0.0613	10
*NHH/Mo-Tp	-	1.973	-1.827	2.825	-4.197	0.340	11
*NH/Mo-Tp	-	1.779	-1.967	2.764	-4.171	0.620	9.995
*NNHHH/Mo-Tp	3.253	1.673	-1.921	2.711	-4.418	0.870	9
*NNHH/Mo-Tp	1.350	1.803	-1.849	2.797	-4.186	0.399	9.9973

Table S7: (-) Integrated crystal orbital Hamiltonian population (-ICOHP) values and the absolute charge spilling from the pCOHP analysis on different systems of the Mo-Tp monolayer.

Systems	-ICOHP (eV/bond)		Abs. Charge Spilling	
	Spin Channel 1	Spin Channel 2	Spin Channel 1	Spin Channel 2
Mo-O	2.21	2.42	14.23 %	11.51 %
Mo-O (O-C-H)	2.28	2.57	14.23 %	11.51 %
Mo-N (N ₂)	1.21	1.24	13.96%	11.35%

Mo-N (*NNH)	4.45	4.55	13.64%	11.64%
--------------------	------	------	--------	--------

Basis Sets: s p d

Table S8: Mulliken Orbital Gross populations (GP) in different adsorbate/Mo-Tp MOF monolayer systems shown between Mo and the nearest N atom.

Systems	Mulliken Orbital Gross population	
	Mo	N
Mo-N (N₂)	5s = 0.27 5p _y = -0.08 5p _z = 0.08 5p _x = 0.04 4d _{xy} = 0.73 4d _{yz} = 1.03 4d _{z²} = 0.90 4d _{xz} = 0.90 4d _{x²-y²} = 0.92 total = 4.79	2s = 1.64 2p _y = 1.20 2p _z = 1.14 2p _x = 1.06 total = 5.04
Mo-N (*NNH)	5s = 0.13 5p _y = -0.07 5p _z = 0.03 5p _x = 0.04 4d _{xy} = 0.76 4d _{yz} = 1.14 4d _{z²} = 0.67 4d _{xz} = 1.37 4d _{x²-y²} = 0.94 total = 4.99	2s = 1.50 2p _y = 1.19 2p _z = 1.16 2p _x = 1.15 total = 5.00

Table S9: Results of the selectivity analysis featuring N₂ adsorption free energy (ΔG_{*N_2}), H adsorption free energy (ΔG_{*H}), and their difference [$\Delta G_{*H} - \Delta G_{*N_2}$].

Adsite	ΔG_{*N_2}	ΔG_{*H}	$[\Delta G_{*H} - \Delta G_{*N_2}]$
Mo	0.17	0.5344	0.3644
C1	0.197	0.084	-0.113
C2	0.183	-0.058	-0.241

Reference:

[S1] J. K. Nørskov *et al.*, "Origin of the overpotential for oxygen reduction at a fuel-cell cathode," *Journal of Physical Chemistry B*, vol. 108, no. 46, pp. 17886-17892, 2004, doi: 10.1021/jp047349j.

[S2] J. G. Howalt, T. Bligaard, J. Rossmeisl, and T. Vegge, "DFT based study of transition metal nano-clusters for electrochemical NH₃ production," *Physical Chemistry Chemical Physics*, vol. 15, no. 20, pp. 7785-7795, 2013, doi: 10.1039/c3cp44641g.

[S3] Webbook.nist.gov. 2022. *NIST Chemistry WebBook*. [online] Available at: <<https://webbook.nist.gov/chemistry/>> [Accessed 28 September 2022].